UNITED NATIONS EDUCATIONAL, SCIENTIFIC AND CULTURAL ORGANIZATION
INTERNATIONAL ATOMIC ENERGY AGENCY
INTERNATIONAL CENTRE FOR THEORETICAL PHYSICS
I.C.T.P., P.O. BOX 586, 34100 TRIESTE, ITALY, CABLE: CENTRATOM TRIESTE

SMR.998b - 3

Research Workshop on Condensed Matter Physics
30 June - 22 August 1997
MINIWORKSHOP ON
SUPERCONDUCTING MESOSCOPIC STRUCTURES

14 - 25 JULY 1997

"Non-equilibrium Josephson-like effects in mesoscopic S-N-S junctions"

N. ARGAMAN
Institute for Theoretical Physics
University of California
Santa Barbara
CA 93106
U.S.A.

These are preliminary lecture notes, intended only for distribution to participants.

Non-equilibrium Josephson–like effects in mesoscopic S-N-S junctions

Nathan Argaman
Institute for Theoretical Physics, University of California, Santa Barbara, CA 93106, USA

(July 2, 1997)

Wide mesoscopic superconducting–normal-metal–superconducting (S-N-S) junctions exhibit Andreev bound states which carry substantial super-currents, even at temperatures for which the equilibrium Josephson effect is exponentially small — the currents carried by different states can cancel each other. This cancelation is incomplete whenever the junctions are driven out of equilibrium, e.g., by a dc voltage. This leads to new effects, similar to the usual dc and ac Josephson effects, but dominated by the second harmonic of the Josephson frequency, which may explain some striking recent experiments. A simple description of these, in the spirit of the Resistively–Shunted–Junction model, is suggested.

PACS numbers: 74.50.+r, 74.40.+k, 74.80.Fp, 73.23.Ps

Introduction:

A class of mesoscopic systems which has recently attracted much attention is that of "Andreev interferometers". These are superconducting–normal-metal–superconducting (S-N-S) junctions in which the spectrum of electronic excitations in the normal-metal part — the Andreev bound states — can be controlled by adjusting the phase difference ϕ between the two superconductors. Remarkably, this ϕ–dependence does not disappear when the temperature T is raised so that the "normal metal coherence length", ξ_N, becomes much smaller than the distance L between the two superconducting electrodes [1]. It is thus necessary to go beyond a simple Ginzburg–Landau type description of proximity effects in the normal material, which emphasizes the variation of the "induced superconducting order parameter" on length scales of order ξ_N. The natural alternative is to concentrate on the energy-dependence of the spectral properties.

In many of the recent experiments [2], the Ohmic conductance of the normal-metal part, $G(\phi)$, was measured through additional normal-metal leads, and was observed to depend periodically on ϕ. Recently, Volkov and Takayanagi [3] have argued that applying a dc voltage $V = (\hbar/2e)d\phi/dt$ to the superconducting electrodes would bring about ac currents in such systems, and they should thus exhibit Shapiro steps in analogy with the conventional ac Josephson effect. It was later shown that the presence of the extra normal leads was necessary in order for such purely dissipative effects to lead to Shapiro steps [4]. In a separate development, Zhou and Spivak [5] discussed non-equilibrium effects, and observed that if the inelastic relaxation rates in the normal-metal part of the system are small, as often occurs in mesoscopic systems (and if there are no additional normal leads which provide rapid relaxation), then an even stronger phase-dependence of the conductance may occur. Here too the emphasis was on dissipative effects, which occur near equilibrium.

The present work considers situations far from equilibrium, in S-N-S junctions in which the equilibrium Josephson effect is negligible because $L \gg \xi_N$, but mesoscopic effects are still strong because $L \ll l_\varphi$ (here l_φ is the dephasing length or coherence length for electrons and holes in the normal material). Thus, it is an extension of the discussion of Ref. [5], but the theoretical picture is different, based on "adiabatically" following the evolution of the Andreev bound states [6], rather than viewing the effect as a Debye mechanism of relaxation. It is shown that when such junctions are driven out of equilibrium (by an applied voltage, microwave radiation, or external noise), they can carry substantial supercurrents, and exhibit effects very similar to the usual dc and ac Josephson effects, but with some unexpected twists.

The fact that non-equilibrium effects tend to enhance superconductivity was discussed extensively in the seventies [7], but in most experiments the enhancement was not large, with the supercurrents and critical temperatures growing by only a few percent or tens of percent under microwave irradiation [8]. Furthermore, the theoretical discussion of S-N-S junctions often used a Ginzburg–Landau description, in analogy with the discussion of other types of superconducting weak links, e.g., constrictions. Here a much simpler approach can be taken, because there is no need to calculate the effect of the non-equilibrium populations on the pair amplitude in the normal material (the pair potential vanishes in any case). Our approach is limited to low voltages, however — we make no attempt to discuss the subgap structure which occurs when eV is comparable to the superconducting gap Δ. The case of a disordered normal metal will be considered; for a discussion of non-equilibrium effects in clean, ballistic systems see Ref. [9].

The main results of the present work are that wide mesocopic S-N-S junctions are dominated by the non-equilibrium effects, and that the phase dependence of the resulting supercurrents are dominated by the second harmonic of the usual Josephson frequency. This will be used below in an attempt to explain some recent experiments; in fact, the behavior of the second harmonics in these experiments served as the major motivation for embarking on the present project. We recall that in the early eighties two *equilibrium* mesoscopic effects were suggested, in which *only* even harmonics would appear (period -halving). In the first case [10] the weak-localization effect on the conductance was evaluated. This amounts to a small correction, of order e^2/h, to the conductance, and should thus be negligible compared to the effects discussed here (as long as the system is in the metallic limit). The second was a certain contribution of electron-electron interactions to the equilibrium Josephson currents [11]. This could be a larger contribution, but it was found that it decays with temperature more rapidly than the basic interaction-less contribution, and would thus not dominate the junction (unless the normal metal N is ferromagnetic).

What happens in equilibrium?

Consider then the electronic spectrum for an S-N-S junction of simple slab geometry, with the N layer having a "width" L (sometimes referred to as the length of the junction) and a diffusion constant D. The low-lying electrons and holes — those with excitation energies ϵ much smaller than the superconducting gap Δ — are confined to the normal-metal layer: an electron with energy $E_F + \epsilon$ with $\epsilon < \Delta$ can enter the superconductor only by pairing with another electron from the Fermi sea at energy $E_F - \epsilon$, and leaving behind a hole, i.e. it is Andreev-reflected into a hole by the N-S interface (we ignore electron interactions in the normal metal). The reverse process, a hole breaking up a Cooper pair and being reflected into an electron, can also occur. These processes are coherent and have associated scattering phase shifts which depend on the phase of the order parameter in the S material, and eventually lead to the formation of quantized states which are coherent mixtures of electrons and holes — generalizations of the Bogolyubov quasiparticles in the superconductor. In an S-N-S system the spectrum of these states depends on the difference ϕ between the phases of the two S electrodes.

An example of such a spectrum is shown in Fig. 1. In principle the spectrum should be calculated from the Bogolyubov - de Gennes equations, but the disorder-averaged density of states can also be calculated from the simpler Usadel equations [12], the standard tool for the description of inhomogeneous disordered superconductors. In the present case it was calculated from an equivalent scattering approach [13]. The results in the figure are for the case with "perfect" S-N boundaries, i.e. electrons and holes which impinge on the N-S boundary Andreev scatter with an amplitude of unit magnitude, and the probability for normal scattering vanishes. Once the density of states $\nu(\epsilon, \phi)$, has been found, the average

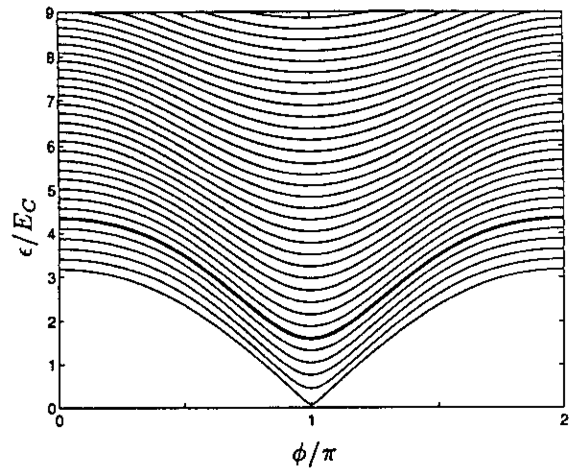

FIG. 1: Energies of Andreev bound states $E_n(\phi)$, as a function of the phase difference between the two superconductors ϕ, for a simple diffusive S-N-S junction. Only the (disorder-averaged) positions of representative levels have been drawn, as the density of states is assumed to be high (the figure also assumes that the superconducting gap, Δ, is much larger than the Thouless energy, E_C). The thick line is a representative curve $E_{\rm rep}(\phi)$ used below.

energy $E_n(\phi)$ of the nth level may be found by integration: $n = \int_0^{E_n} \nu(\epsilon, \phi)\, d\epsilon$. Note that although the calculation actually gives the space-dependent local density of states, only its spatial integral, $\nu(\epsilon, \phi)$, appears in our considerations.

At the Fermi surface E_F, and for $\phi = 0$, a gap is induced in the normal material by the proximity effect [14]. Further away, the electrons and holes have different wavefunctions or different scattering properties, because of the difference in wavenumbers between the energies $E_F + \epsilon$ and $E_F - \epsilon$. This difference is significant if it is larger than the Thouless energy E_C, which is defined as $\hbar$ over the typical time it takes a particle to cross the normal metal, $E_C = \hbar D/L^2$. When $\epsilon \gg E_C$, the density of states is not strongly affected by the proximity effect, and approaches its normal-state value, $1/\delta$, where δ is the mean level spacing. We assume that δ here is negligibly small and the spectrum is continuous, but it is still convenient to speak in terms of contributions of individual levels E_n.

The proximity-induced mini-gap extends in the present case up to an energy $E_g \simeq 3.1 E_C$ for $\phi = 0$ [for a particular realization of the disorder, the energy of the first level deviates from the averaged $E_g(\phi)$ only by an amount of order δ]. When ϕ is non-zero, the two superconductors are "not aligned" and a smaller mini-gap is induced; when $\phi = \pi$ one finds $E_g = 0$. The details of the spectrum are different for other cases — for example E_g is smaller if the N-S surfaces are not perfect — but for the purposes of the present work all we need to know is that the spectrum depends on ϕ, and the details of the $E_n(\phi)$ curves will only affect the details of the results. Thus, ballistic systems with an elastic mean free path l_{el} of the order of L (and a Fermi velocity v_F and a Thouless energy $E_C = \hbar v_F/L$) are also expected to behave similarly. On the other hand a perfectly clean system of separable geometry with perfect N-S boundaries may not, because in such systems the $E_n(\phi)$ curves can cross each other, leading to somewhat different non-equilibrium effects [9].

The fact that E_n depends on ϕ directly implies the existence of currents, $I = (2e/\hbar)(dE_n/d\phi)$ per electron in the nth state. This may be understood either as the expectation value of the current operator, or by equating the amount of energy $IVdt$ expended by an external source with the energy stored in the electrons $\sum dE_n$, and making use of the Josephson relationship $d\phi = (2e/\hbar)Vdt$. For each n there is also a state with energy $-E_n$, which carries the opposite current. The total supercurrent through the junction is thus

$$I_S = -\frac{2e}{\hbar}\sum_n \frac{dE_n}{d\phi}(1-2f) , \tag{1}$$

where I_S denotes the supercurrent, f is the occupation probability for the state E_n, and $1-f$ is the occupation of the $-E_n$ state [15] (the summation over spin is included in the sum over n, and for a continuous spectrum the summation may be replaced by an integration).

In thermal equilibrium, f is given by the Fermi–Dirac distribution, $f_{\text{eq}} = 1/\left(1+\exp(\epsilon/T)\right)$, where we have set $k_{\text{B}} = 1$. The expression for the supercurrent then becomes

$$I_{\text{eq}}(\phi) = \int_0^\infty d\epsilon\, j(\epsilon,\phi)\tanh(\epsilon/2T) , \tag{2}$$

where $j(\epsilon)$ denotes the Josephson current per unit energy, $j(E_n,\phi) \propto \nu(E_n,\phi)(dE_n/d\phi)$. We are interested here in the high temperature case, $T \gg E_C$, which is equivalent to the condition $\xi_N \ll L$ mentioned above (here $\xi_N = \sqrt{\hbar D/T}$ by definition). The fact that I_{eq} decays exponentially with increasing temperature is not obvious here, as $j(\epsilon)$ is essentially independent of temperature in the mesoscopic regime, $L \ll l_\varphi$, so the integrand does not decay rapidly with rising T. Instead, the small values of I_{eq} are a result of a cancelation between positive and negative values of the integrand — $j(\epsilon)$ oscillates as a function of ϵ, with an envelope which decays rapidly when ϵ becomes much larger than E_C (in order to see the first oscillation on a plot such as Fig. 1, one must go much higher in ϵ, and magnify its scale by an order of magnitude).

The fact that I_{eq} can become exponentially small is clearer if one extends the integration in Eq. (2) to $-\infty$ (the integrand is even), and uses contour integration in the complex ϵ plane. A positive imaginary part of ϵ corresponds physically to dephasing, i.e. a finite l_φ, and this implies that $j(\epsilon)$ is analytic in the upper half of the complex plane. The only poles are thus due to the tanh factor, and one finds that $I_{\text{eq}} = 2\pi i T\sum_1^\infty j(i\omega_n)$, where $\omega_n = (2n-1)\pi T$ are the Matsubara frequencies. The precise cancelation of the oscillatory integrand is thus related to the fact that $j(\epsilon)$ decays exponentially for large positive imaginary values of ϵ, i.e. for $l_\varphi \ll L$. In fact, for $T \gg E_C$ one may argue that the contribution of the first Matsubara frequency dominates, and there is no need to evaluate $j(\epsilon)$ at more than one point. Likewise, the pair amplitude may be evaluated at $\epsilon = i\omega_1$, and this directly leads to the picture of its decaying on the length scale ξ_N. This argument is very general — true for both dirty and clean systems, etc. — but it does not hold for all aspects of the proximity effect (e.g. not for the conductance, as emphasized in Ref. [3]), and it does not hold in non-equilibrium situations. This last limitation is very important for junctions of the type considered here, because of the strong phase–dependence of the spectrum (Fig. 1), and the slow inelastic relaxation rates (e.g. large l_φ) characteristic of the mesoscopic regime. Thus, whenever a voltage is applied to the junction, the spectrum becomes time dependent and the system is driven out of thermal equilibrium, at least to some extent.

Non-equilibrium model

The simplest possible model for a (semi)quantitative description of non-equilibrium effects is the relaxation time approximation,

$$\frac{df}{dt} = -\frac{1}{\tau_E}(f - f_{\text{eq}}) , \tag{3}$$

where the derivative is taken at constant n, f_{eq} is time-dependent through the ϕ-dependence of E_n (Ref. [16]), and τ_E is taken as a constant. Note that this is a very approximate description of relaxation by electron-phonon or electron-electron interactions: it not only excludes a possible dependence of τ_E on ϵ, but also ignores the presence of the phase-dependent gap in the electronic spectrum.

Rather than attempting a more sophisticated description of relaxation, we argue that the deviation of f from f_{eq} is small for large energies (because the corresponding E_n curves are flat) and that therefore one may use a value of τ_E representative of relaxation at $\epsilon \sim E_C$. Furthermore, the different E_n curves at these energies are rather similar to each other — a simple shift in ϵ is insignificant if $T \gg E_C$ — and therefore one may choose one of these curves as a representative, $E_{\text{rep}}(\phi)$ (it is easy to check this approximation by comparing to a model which retains the n dependence). We thus write the supercurrent as

$$I_S = I_{\text{eq}}(\phi) + 2\frac{2e}{\hbar}N\frac{dE_{\text{rep}}}{d\phi}(f - f_{\text{eq}}) , \tag{4}$$

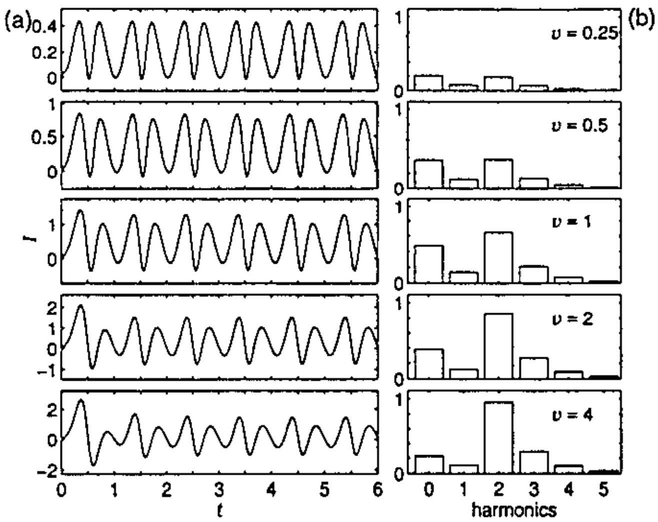

FIG. 2: (a) Current (in units of $I_{\rm neq}$) as a function of time (in units of the corresponding Josephson period), and (b) amplitudes $|I_k|$ (with $k \geq 0$) of the harmonic decomposition of the same data at times $t \gg \tau_E$. Results are shown for five different values of the voltage, labeled by $v = (2e/\hbar)V\tau_E$.

where $I_{\rm eq}(\phi)$ is the equilibrium supercurrent, and N is the number of levels represented by $E_{\rm rep}$, which is of order E_c/δ. Note that the cancelation which affected the integral expression for I_S in equilibrium cannot recur for the nonequilibrium part, because the decreasing oscillations of $j(\epsilon)$ are here multiplied by a decreasing function $f - f_{\rm eq}$, rather than the increasing $1-2f_{\rm eq}$ factor.

(i) *ac effects*

The model consisting of Eqs. (3) and (4) generates ac super-currents when a dc voltage is applied to the junction, $d\phi/dt = 2eV/\hbar = \text{const.}$, as shown in Fig. 2. We have chosen $E_{\rm rep} = 3.4E_C\sqrt{1+0.7\cos(\phi)}$ as the representative energy — this simple form fits the thick line of Fig. 1 within a few percent (the corresponding value of N is $10E_C/\delta$, including a factor of 2 for spin). We have also used the $T \gg E_C$ condition to take $I_{\rm eq} = 0$ and $f_{\rm eq} = \frac{1}{2} - E_{\rm rep}/4T$. The current is plotted in the figure in units of $I_{\rm neq}$, defined below, which is essentially the maximum amplitude of the $-\sin(2\phi)$ component of the current, attained in the $V \to \infty$ limit. The results with the full set of $E_n(\phi)$ curves are very similar to those shown — the amplitudes of the harmonics in 85% of the cases shown agree within less than 15%. Thus the approximation of using a single $E_{\rm rep}(\phi)$ rather than a multitude of $E_n(\phi)$s should not introduce errors larger than those associated with the relaxation time approximation, Eq. (3).

Note that in all cases the second harmonic of the usual Josephson frequency dominates the ac currents. This occurs because the current of Eq. (4) is a product of two factors, $dE_{\rm rep}/d\phi$ and $(f - f_{\rm eq})$, each of which oscillates with the Josephson frequency. In fact, in the simplest case $E_{\rm rep} \propto \cos(\phi)$, and the current gradually crosses over from a $\sin^2(\phi)$ behavior to $-\sin(2\phi)$, as the voltage is increased, with only the dc component and the second harmonic present. This simple case may be used to describe junctions with $L \sim l_\varphi$ or with significant time reversal symmetry breaking (e.g. scattering by magnetic impurities), because in such cases one would expect the $E_n(\phi)$ curves to be considerably "softened".

The results simplify, of course, in the limits of small or large voltages. In the first case we return to the results of Ref. [5] (see also Ref. [7]),

$$f = f_{\rm eq} - \tau_E \frac{2e}{\hbar} V \frac{df_{\rm eq}}{d\phi} + O(V^2)\,, \qquad (5)$$

and thus

$$I_S = \left(\frac{2e}{\hbar}\right)^2 \frac{N\tau_E V}{2T} \left(\frac{dE_{\rm rep}}{d\phi}\right)^2 + O(V^2)\,, \qquad (6)$$

where again the multiplication by N may be replaced by a summation over $(dE_n/d\phi)^2$ for a more accurate description. This gives an additive phase–dependent contribution to the Ohmic conductance of the junction, due to the dissipative relaxation of the slightly non-equilibrium distribution present in the junction at each instant.

In the opposite limit of high dc voltages, we may replace f by the time-averaged or phase-averaged $f_{\rm eq}$:

$$\bar{f} = \frac{1}{2\pi} \int_0^{2\pi} d\phi\, f_{\rm eq}\left(E_{\rm rep}(\phi)\right) + O(1/V)\,. \qquad (7)$$

In this limit the response of the junction is purely "reactive", with the oscillating current flowing sometimes in the direction of the applied voltage, and sometimes in the opposite direction. In fact, the time-averaged dissipated power approaches a constant value P_{max} at large V, and so the dc component of the current decreases as P_{max}/V.

The results shown in the figure resemble the "usual" ac Josephson effect, albeit with a richer harmonic content. Such ac Josephson oscillations are usually observed experimentally by applying an ac drive (i.e. microwave radiation) in addition to the dc drive, and looking for so–called Shapiro steps: the I–V curves exhibit phase–locking when the Josephson frequency matches the frequency of the external drive (the voltage is locked to the microwave frequency over a range of values of the current). In the simplest analysis, one assumes $\phi(t) = \phi_0 + (2e/\hbar)V_{\rm dc}t + (2eV_{\rm ac}/\hbar\omega)\sin(\omega t)$, and finds the time-averaged, dc component of the current, $I_{\rm dc}$.

Given the harmonic content of the oscillations displayed in Fig. 2, the results for the $\tau \to \infty$ limit are generally not surprising. Specifically, for the simplest $E_{\rm rep} \propto \cos(\phi)$ case, one finds Shapiro steps whenever $(4e/\hbar)V_{\rm dc}$ is equal to an integer multiple of ω.

In this case f develops a non-zero time-averaged value only for the even steps, $f \propto \cos(\phi_0) J_{v_{dc}}(v_{ac})$, where J denotes the Bessel function, and v_{dc} and v_{ac} denote the scaled voltages, e.g. $v_{dc} = (2e/\hbar)V_{dc}/\omega$. The current I_S has two contributions, one proportional to $f\sin(\phi)$ and the other to $-\sin(2\phi)$, and thus $I_{dc} \propto \sin(2\phi_0)\left(J^2_{v_{dc}}(v_{ac}) - J_{2v_{dc}}(2v_{ac})\right)$. For the odd Shapiro steps $f = 0$ and $I_{dc} \propto -\sin(2\phi_0) J_{2v_{dc}}(2v_{ac})$, which differs from the usual results for Shapiro steps only by the doubling of the Josephson frequency and a sign.

For a more general $E_{rep}(\phi)$, Shapiro steps exist also when ω (or an integer multiple thereof) is equal to $k(2e/\hbar)V_{dc}$ for other harmonics $k \neq 2$, and the magnitudes of these steps are related to those of the different harmonics seen in Fig. 2. In this case many of the steps (including the integer steps) have $\sin(k\phi_0)$ contributions with several different ks, and the amplitudes for the different k harmonics vanish at different values of V_{ac}. Thus the total magnitudes of the Shapiro steps oscillate with V_{ac}, but no longer have zeros.

It is interesting to note that in the limit of small τ_E, the magnitudes of the Shapiro steps decrease quadratically, as $\tau_E^2 \omega V_{ac}$, and not linearly (as $\tau_E V_{dc}$) as do the ac currents themselves. This is due to the purely dissipative nature of the non-equilibrium currents in this limit, $I_S \propto G(\phi)V$, to first order in τ_E. The fact that the dc current, $\int I\, dt$, can be written as a phase integral with no time dependence, $\int G(\phi)d\phi$, directly implies that no Shapiro steps will be manifest to first order in τ_E (see Ref. [4]).

(ii) *I–V curves*

So far, with the exception of the last paragraph, we have considerd the voltage $V(t)$ as given. However, in most experimental set-ups the junction is driven by a circuit which is better represented by a current bias. It is thus desirable to have a more general model of the junction. An obvious route is to generalize the well-known resistively–shunted–junction (RSJ) model [17]. The current is written as a sum of components, $I = I_S + I_N + I_F$, where I_N is the normal current and I_F is a fluctuating noise component (we are considering overdamped junctions, with no capacitive term or displacement current). The normal current can be written simply as $I_N = G_N V$ where G_N is the normal conductance. This is of course an approximation, and is valid only as long as the voltages are small enough, as discussed in the next paragraph.

Our assumption that the occupations f follow the states E_n "adiabatically" ignores some effects which become important at large voltages V. One way to estimate these effects is to say that in a time τ_E, a particle can cross the junction $\tau_E E_C/\hbar$ times, each time gaining or loosing an energy eV randomly due to the time-dependent phases associated with Andreev reflections off the N-S surfaces at the two sides. In order for our adiabatic considerations to be valid, this must not add up to an amount of order E_C, which restricts us to small voltages $eV \ll \sqrt{E_C\hbar/\tau_E}$. Another way of arriving at this limitation is to think of the dissipative conductance as introducing a diffusive term in the evolution of the occupations f (Ref. [18]). The magnitude of this $D_E(\partial^2 f/\partial\epsilon^2)$ term is $D_E(\epsilon,\phi) \sim \delta G_N V^2$, because the power absorbed by the electrons, $\int \nu d\epsilon (\partial f/\partial t)\epsilon$, is $\sim G_N V^2$. The ϵ and ϕ dependence of D_E, which are the topic of study in Ref. [1], are always less than a factor of 2 and thus unimportant for the purpose of the present estimate. Ignoring this energy–diffusion term compared to the relaxation term is justifiable if $\tau_E D_E \ll E_C^2$, which again leads to the requirement of small voltages $eV \ll \sqrt{E_C\hbar/\tau_E}$, as above.

We thus describe the normal current by a simple conductance $I_N = GV$, where G is given by an energy–averaging of D_E. The conductance can be approximated by its normal value G_N (i.e. its value in the absence of superconducting proximity effects), because the width of the averaging window is given by the temperature, and the diffusion "constant" D_E attains its normal value at energies $\epsilon \gg E_C$. Note that including the D_E term in the equation for $\partial f/\partial t$ allows one to go beyond the low voltage region (i.e. to include heating effects), at the price of having to contend with a partial differential equation — the specifics of $D_E(\epsilon,\phi)$ is another "spectral property" which can be extracted from the detailed space-dependent Green's functions obtained in Ref. [13]. On the other hand, a study of voltages comparable to or higher than E_C/e would require much more effort, because in that case the temporal and spatial dependencies of the Green's functions would become intertwined.

It is convenient to rewrite the model in a way which explicitly gives the time derivatives of ϕ and f:

$$\frac{d\phi}{dt} = \frac{2e}{\hbar G_N}\left(I - I_{neq} 2\frac{d\hat{E}}{d\phi}(\hat{E} - \hat{f}) - I_F\right) \quad (8)$$

$$\frac{d\hat{f}}{dt} = \frac{1}{\tau_E}\left(\hat{E} - \hat{f} + J_F\right) . \quad (9)$$

Here $\hat{E}$ is a linearly rescaled version of $E_{rep}(\phi) = A\hat{E} + B$, with A and B chosen such that $\hat{E}$ decreases from 1 to -1 as ϕ goes from 0 to π. Likewise, $\hat{f}$ is used instead of $f = \frac{1}{2} - (A\hat{f} + B)/4T$. The rescaling factors are included in the coefficient $I_{neq} = (2e/\hbar)NA^2/4T$. For the system under discussion, $A \simeq 1.3E_C$ and the energy scale corresponding to I_{neq} becomes $E_{neq} = (\hbar/2e)I_{neq} \simeq 4.1E_C^3/\delta T$. Remarkably, this is only a factor of $E_C/3.5T$ smaller than the energy scale corresponding to the critical current for the same junction at $T = 0$. The fluctuating component of the current, I_F, and of the change in occupation, J_F, are used to describe noise, and will be set to 0 initially, in order to discuss the noiseless case ($T \ll E_{neq}$).

The predictions for the I–V curves in this non-equilibrium model are shown in Fig. 3. Here a sim-

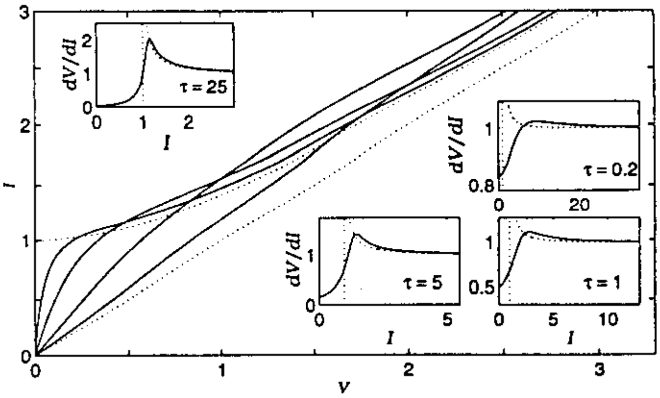

FIG. 3: The I–V curves and differential resistances (insets) for the non-equilibrium model. The current is in units of $I_{\rm neq}$, and the voltage in units of $V_{\rm neq} = I_{\rm neq}/G_N$. Results are given for four different values of the relaxation time τ_E, increasing upwards in the left part of the main figure, and indicated in the insets in units of $\hbar/2eV_{\rm neq}$. The results of the RSJ model with $I_c = I_{\rm neq}$ are drawn dotted for comparison, as is the diagonal $I = G_N V$.

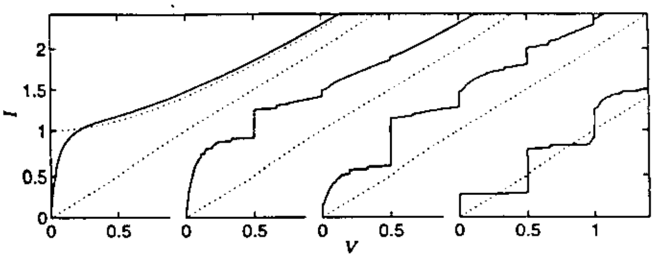

FIG. 4: The dc I–V curves in the presence of an ac current bias, $I_{\rm ac} = 0, 0.5I_{\rm neq}, I_{\rm neq}, 2I_{\rm neq}$, from left to right. The displayed results are for $\omega = 2eV_{\rm neq}/\hbar$ and $\tau_E = 25\hbar/2eV_{\rm neq}$ (the curve at the extreme left is the "unirradiated" result of Fig. 3).

ple dc current, $I(t) = $ const., was assumed, and the $E_{\rm rep}(\phi)$ curve of Fig. 2 was used [as the harmonic content is not apparent in these curves, they are not sensitive to the specific choice of $E_{\rm rep}(\phi)$]. The curves at large values of τ_E remarkably resemble the I–V plots of the usual RSJ model. The slope of the curve near the origin — the zero–bias conductance — is not infinite though, it is equal to $G_N + \tau_E(2e/\hbar)I_{\rm neq}$, or simply $1+\tau$ in the units used in the figure. Note that the low voltage condition discussed above, when expressed in terms of the unit used in the figure, $V_{\rm neq} = I_{\rm neq}/G_N$, reads $eV \ll \sqrt{E_C\hbar/\tau_E} \sim eV_{\rm neq}(T/E_C)\sqrt{\hbar/E_C\tau_E}$. Thus, for a particular junction (and a particular temperature, etc.), the corresponding curve in the figure is relevant only up to a point determined by the ratio of the two large parameters T/E_C and $\sqrt{E_C\tau_E/\hbar}$.

The finite zero–bias conductance exhibited in the figure prompts us to compare these curves with those obtained in the RSJ model when noise is taken into account, which share this feature [17]. In contrast to the cases of thermal or non-thermal noise in the usual RSJ model, the different curves of Fig. 3 cross each other. More precisely, as the curves approach the diagonal when $\tau_E \to 0$, the maximum of the differential resistance shifts to higher and higher currents relative to $I_{\rm neq}$, and occurs at $I \simeq G_N\hbar/e\tau_E$. Thus it is not possible to simply "read off" the current scale $I_{\rm neq}$ (or voltage scale $V_{\rm neq}$) of the present model from the position of this maximum, unless τ_E is large.

The predictions for Shapiro steps are also modified when a current–biased rather than a voltage–biased situation is considered, see Fig. 4. Two noteworthy changes relative to the voltage biased case are: (a) the general tendency of the I–V plot to approach the diagonal when $V_{\rm ac}$ becomes substantial; and (b) the "squeezing", or decreasing size, of the Shapiro steps under low frequency conditions, where a naive use of the voltage–biased results would give overlapping current ranges for successive steps. These changes are similar to the corresponding ones in the standard RSJ model [17].

(iii) *noise*

We now turn to the consideration of thermal and external noise in such junctions, i.e. introduce the fluctuating parts I_F and J_F in Eqs. (8) and (9). These two equations can be derived from a free energy function $F(\phi,\hat f) = E_{\rm neq}(\hat E - \hat f)^2 - (\hbar/2e)I\phi$, which generalizes the well-known tilted washboard potential. The "potential landscape" function $F(\phi,\hat f)$ may be visualized as a winding valley, with a parabolic cross–section in the $\hat f$ direction. The bottom of the valley is described by the periodic $\hat E(\phi)$ curve, and for $I = 0$ it has zero overall slope. At a finite temperature T, points up to a height of order T up the walls of the valley will be occupied. Such thermal fluctuations are described mathematically by the correlators $\langle I_F(t)I_F(0)\rangle = 2TG\,\delta(t)$ and $\langle J_F(t)J_F(0)\rangle = (\tau_E T/E_{\rm neq})\,\delta(t)$, in accordance with the fluctuation–dissipation theorem.

This description of thermodynamic equilibrium holds regardless of whether $\hat f$ is a "fast" variable, with a small value of τ_E, or a "slow" variable with large τ_E. In the first case (and also in cases where ϕ is kept fixed by an external superconducting circuit) we can integrate out $\hat f$. As it fluctuates in a parabolic potential with a minimum at $F = 0$ regardless of ϕ, the resulting free energy will be constant as a function of ϕ and uninteresting — the fact that the minimum of the parabola is at a ϕ–dependent point, $\hat f = \hat E$, becomes immaterial. It is still interesting to note the size of the fluctuations $\delta\hat f$ and their effects on the supercurrent: $\delta\hat f^2 \sim T/E_{\rm neq}$ and $\delta I_S = 2I_{\rm neq}(d\hat E/d\phi)\delta\hat f$. The first implies $\delta f^2 \sim 1/N$, as should be expected of a group of N levels with f near

$\frac{1}{2}$. The second implies $\delta I_S^2 \sim I_{\rm neq}(2e/\hbar)T(d\hat{E}/d\phi)^2$, with a correlation time of τ_E. This differs from the fluctuations in I_F by a factor of $\tau_E(2e/\hbar)V_{\rm neq}$, which is the same as the factor appearing in the zero-bias conductance displayed in Fig. 3. As pointed out in Ref. [19] for clean junctions, these supercurrent contributions to noise and conductance are related by the fluctuation–dissipation theorem, and indeed one finds the same phase dependence, $(d\hat{E}/d\phi)^2$, in both cases.

In the opposite case of large τ_E we can think of ϕ as the fast variable, and integrate it out. The resulting free energy, $\tilde{F}(\hat{f})$, will not be featureless, but will also not be very steep. In fact, it is easy to find the probability density, $\propto \exp(-\tilde{F}(\hat{f})/T)$, by projecting this picture of a "water–filled winding river" on to the $\hat{f}$ axis. It is a convolution of a simple Gaussian [because $F(\phi, \hat{f})$ is parabolic in $\hat{f}$], and a distribution proportional to $|d\hat{E}/d\phi|^{-1}$, which is sharply peaked at $\hat{f} = \pm 1$. For the $\hat{E} = \cos(\phi)$ case, this distribution is $(1-\hat{f}^2)^{-1/2}$, whereas for other cases it is asymmetrical, with the maximum at $\hat{f} = 1$ being more prominent. At low temperatures we may use the width of the Gaussian, $\sim \sqrt{T/E_{\rm neq}}$ to cut off the inverse–square–root divergence. This gives a ratio of the maxima to the local minimum (around $\hat{f} = 0$) probability densities $\sim (E_{\rm neq}/T)^{1/4}$, and the variation of $\tilde{F}(\hat{f})/T$ is logarithmic in this ratio.

As long as the noise is purely thermal, the situation does not become very interesting: when one "tilts the valley" by imposing a finite current I, one finds that the voltage, or rate of phase–slip, is always enhanced relative to the zero-temperature case. However, whereas the noise in $\hat{f}$ is driven by the thermalization of the electrons at their temperature T, the noise in the phase ϕ may be larger than thermal. This occurs if the dominant source of current noise in the circuit is not the thermal noise in the S-N-S junction itself. One may describe such high–frequency noise by introducing a "phase temperature" T_ϕ, such that $T_\phi > T$ (low–frequency noise would affect the dynamics of $\hat{f}$ as well, and not only the dynamics of ϕ). If τ_E is long, we may integrate out the ϕ variable as above, resulting in a $\tilde{F}(\hat{f})$ curve with variations on the scale of T_ϕ. When we now solve for the dynamics of the $\hat{f}$ variable, we find it *strongly* attracted to the minima of the $\tilde{F}$ curve, because the thermal energy T is relatively small [20]. Thus, the variable $\hat{f}$ tends to get trapped near the extremal values of $\hat{E}$, and phase-slip occurs only in discrete events and is strongly suppressed.

This suppression of phase-slip occurs also when a small current I is present. Thus, the zero-bias conductance of the junction *grows* with external noise, at first, see the inset in Fig. 5. Although the zero-bias conductance can grow substantially for large τ_E, this affects only the very low–current portion of the I–V curve, and at higher currents the effect of noise is as expected (the main figure). Note that a modest amount of thermal noise can wash

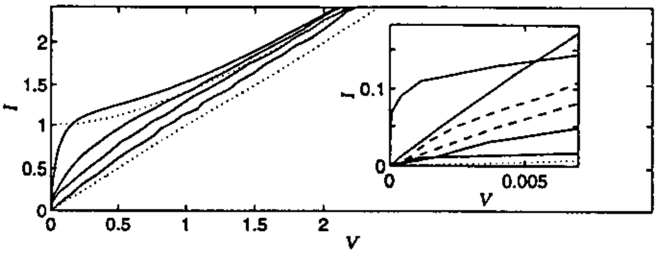

FIG. 5: The I–V curves in the presence of external noise $T_\phi = 0, 0.25E_{\rm neq}, 0.5E_{\rm neq}, E_{\rm neq}$, from top to bottom. The waviness of the curves reflects the accuracy due to the finite numerical integration time (again, we have chosen $\tau_E = 25\hbar/2eV_{\rm neq}$ and reproduced the $T_\phi = 0$ of Fig. 3). Inset: the same curves on a much expanded scale, such that the $T_\phi = 0$ curve appears diagonal and the dotted $I = G_N V$ line is near the horizontal axis. Note that the $T_\phi = 0.25E_{\rm neq}$ curve crosses the $T_\phi = 0$ one, and appears to have a "critical current" of $0.1 I_{\rm neq}$ (of course, it also reveals a finite zero-bias conductance upon further magnification). The dashed lines show that thermal noise counteracts this effect: here $T = 0.05$ (top) and 0.25 (bottom), with T_ϕ kept at 0.25 (for all other curves $T = 0$, see text).

away this effect (see dashed lines in inset). A detailed survey of the results for different values of T_ϕ, T, τ_E and I is beyond the scope of the present work.

Experiments

We now finally turn to the experimental motivation for this work. Observations of Josephson–like effects, with a "strange" tendency for dominance of the second harmonic, were recently made in a one-dimensional array of long wide S-N-S junctions, where the normal material was an In-As quantum well, and the superconductor was Niobium [21,22]. Direct motivation was given by the ac measurements [22], which showed Shapiro steps of various (sub)harmonics. Surprisingly, one of the Shapiro steps was observable even at relatively high temperatures, 8K in one case (the T_c of the sputtered Niobium used was about 8.5K). This was not the fundamental Shapiro step, but the one with ω corresponding to the second harmonic of the Josephson frequency. At such high temperatures one can perhaps argue that the non-equilibrium effect is strong compared to the equilibrium Josephson coupling. Indeed, in the same experiments the superconducting effects gradually disappeared when the frequency was increased beyond $\sim 3 \times 10^{11}$Hz, which if interpreted as the inverse of the time the electrons spend *en route* from one S electrode to the other, corresponds to a value of E_C of the order of 10K.

A detailed comparison between the present theory and the existing experiments is complicated, because the conditions $T \gg E_C$, $L \ll l_\varphi$, and $eV \ll \sqrt{E_C\hbar/\tau_E}$ are only marginally met in the experiments, at best. Furthermore, the experiments used a rather clean quantum well ($l_{el} \simeq 6\mu$m before processing, compared to $L \simeq 0.4\mu$m), and so the detailed results obtained here are not directly applicable. However, the simplicity of the present model allows for modifications which could perhaps alleviate these concerns, provided that the several new parameters which would be introduced by such modifications were independently determined. Further experiments, aimed at clarifying the situation, are currently underway. An interesting possibility is to measure the inelastic relaxation rate of the Andreev bound states directly, using a time–resolved pump–probe experiment [23].

The dc measurements [21] of zero–bias conductances in this system showed a periodicity in magnetic field corresponding to a flux of $\pi\hbar/2e$, or half a flux quantum, per junction. These measurements were made at lower temperatures, $\sim 4K$, and were originally interpreted in terms of a superlattice of Josephson vortices, with the number of vortices in the combined area of two neighboring junctions increasing by one unit per period. However, it is arguably more natural to interpret the results in terms of Josephson half-vortices, which would arise if the present non-equilibrium model were generalized to the case of long junctions. Here "long" refers to the direction perpendicular to the current flow, which in the experiment was about 100 microns. Clearly, the populations f of the Andreev bound states may equilibrate in the lateral direction, and one would need to identify the length–scale over which such equilibration is effective.

There are two distinct possibilities for Josephson half–vortices to evolve in such a junction: firstly, if one looks at distances much larger than the equilibration distance, the different segments of the junction become independent of each other. If then the system is driven by some noise, as in the $T_\phi \gg T$ situation described above, one should find different segments trapped in different minima, with $\hat{f}$ near 1 or near -1, and in the region between such segments an amount of magnetic flux equal to half a flux quantum (or an odd multiple thereof) would be trapped. The opposite case of fast lateral equilibration is more difficult to analyze, because it is no longer clear that the occupations of different levels can be represented by a single $E_{\rm rep}$ curve. However, it is interesting to note that if for any reason one finds that $\hat{f} \simeq 0$, then the ϕ variable would see a "washboard potential" with minima whenever $\hat{E}$ is near zero, i.e. near all *odd* multiples of $\pi/2$, again resulting in "Josephson half–vortices". This situation is similar to the one involving a ferromagnetic N material, considered in Ref. [11], and indeed a detailed comparison with the experiment would require a careful evaluation of the effects of interactions (a straightforward application of the formulae of Ref. [11] indicates that this particular interaction contribution should be negligible for the experimental geometry, even at zero temperature). The study of these intriguing possibilities, and their possible relation with the experiments, is left for future work.

Conclusion

In summary, we have found that a wide mesoscopic S-N-S junction which carries an exponentially small Josephson current under thermodynamic equilibrium conditions, i.e. one with $L \gg \xi_N$, may still exhibit effects very similar to both the dc (Fig. 3) and the ac (Fig. 2) Josephson effects. The non-equilibrium conditions may be brought about by irradiating the junction with microwaves, connecting it to a noisy circuit, or simply applying a voltage. The magnitude of the new effects decays only as $I_{\rm neq} \propto E_C/T$, and not exponentially with temperature as does the equilibrium critical current I_c (they also require relatively slow relaxation rates, $1/\tau_E$, but such slow rates are natural in the mesoscopic regime). The new effects have the signature of being dominated by the second harmonic of the Josephson frequency, and may have already been observed.

Acknowledgements

I would like to thank S.J. Allen, J.G.E. Harris, H. Kroemer, K. Lehnert, B. Spivak and F. Zhou for fruitful discussions. This work was supported by NSF grants No. PHY94-07194 and No. DMR93-08011.

---

[1] H. Courtois, Ph. Gandit, D. Mailly, and B. Pannetier, Phys. Rev. Lett. **76**, 130 (1996); and references therein.

[2] See, e.g., V.T. Petrashov, V.N. Antonov, P. Delsing, and T. Claeson, Phys. Rev. Lett. **74**, 5268 (1995).

[3] A.F. Volkov and H. Takayanagi, Phys. Rev. Lett. **76**, 4026 (1996).

[4] J.G.E. Harris, N. Argaman, and S.J. Allen, Phys. Rev. Lett. **78**, 2678 (1997); A. F. Volkov and H. Takayanagi, Phys. Rev. Lett. **78**, 2679 (1997).

[5] F. Zhou and B. Spivak, Report No. cond-mat/9604185.

[6] D. Averin and A. Bardas, Phys. Rev. B **53**, R1705 (1996), have introduced this approach for the case of a short single–channel junction, with a single Andreev bound state. The justification of its use for the present case, with a dense spectrum of many overlapping states, appears below.

[7] M. Tinkham *Introduction to Superconductivity*, 2nd ed., Chap. 11 (New York, McGraw-Hill, 1996).

[8] For an exception, see J.M. Warlaumont, J.C. Brown, T. Foxe, and R.A. Buhrman, Phys. Rev. Lett. **43**, 169 (1979).

[9] See U. Gunsenheimer and A.D. Zaikin, Phys. Rev. B **50**, 6317 (1994); and references therein.

[10] B.Z. Spivak, and D.E. Khmelnitskii, Pis'ma Zh.E.T.F. **35**, 334 (1982) [JETP Lett. **35**, 412 (1982)].
[11] B.L. Altshuler, D.E. Khmelnitskii, and B.Z. Spivak, Solid State Comm. **48**, 841 (1983).
[12] K. Usadel, Phys. Rev. Lett. **25**, 507 (1970).
[13] N. Argaman, manuscript in preparation [this is an outgrowth of N. Argaman, Europhys. Lett. **38**, 231 (1997)].
[14] For a recent discussion, see J.A. Melsen, P.W. Brouwer, K.M. Frahm, and C.W.J. Beenakker, Europhys. Lett. **35**, 7 (1996); see also W. Belzig, C. Bruder, and G. Schon, Phys. Rev. B **54**, 9443 (1996). Our results for the spectral and equilibrium properties, such as $E_g \simeq 3.1 E_C$, agree quantitatively with earlier works such as these.
[15] Situations of "branch imbalance" [7], for which the occupations of the E_n and the $-E_n$ levels are not necessarily simply related, do not arise in the context of the present work [see Eq. (3)].
[16] Alternatively, one may use a time-independent $f_{\rm eq}(\epsilon)$, and replace $\frac{df}{dt}$ by $\frac{\partial f}{\partial t}\big|_\epsilon + \frac{dE_n}{d\phi}\big|_{E_n=\epsilon} \frac{d\phi}{dt}\frac{\partial f}{\partial \epsilon}$.
[17] See, e.g., *Dynamics of Josephson Junctions and Circuits*, K.K. Likharev (Gordon and Breach, New York, 1986).
[18] See, e.g., M. Wilkinson and E.J. Austin, Phys. Rev. A **46**, 64 (1992).
[19] A. Martin-Rodero, A Levy Yeyati, and F.J. Garcia-Vidal Phys. Rev. B **53**, R8891 (1996); See also D. Averin and H.T. Imam, Phys. Rev. Lett. **76**, 3814 (1996).
[20] Note that even in the $T \to 0$ limit, there is still some noise in the evolution of $\hat{f}$, indirectly induced by T_ϕ.
[21] M. Thomas, H.-R. Blank, K.C. Wong, C. Nguyen, H. Kroemer, and E.L. Hu, Phys. Rev. B **54**, R2311 (1996).
[22] H. Drexler, J.G.E. Harris, E.L. Yuh, K.C. Wong, S.J. Allen, E.G. Gwinn, H. Kroemer, and E.L. Hu, Surf. Science, **361-362**, 306 (1996).
[23] S.J. Allen, private communication.